Electronic Supplementary Information for

A gold nanoparticles-loaded MoS_2 nanosheets with peroxidase-like and pyranose oxidase-like activities for bio-enzyme-free visual detection of glucose, xylose and galactose

Shilan Fu[†‡], Junfeng Liu[†], Siqi Wu[†], Lin Zhang[†], Xu Zhang[*†], FengFu Fu[*†]

[†]Key Laboratory for Analytical Science of Food Safety and Biology of MOE, Fujian Provincial Key Lab of Analysis and Detection for Food Safety, College of Chemistry, Fuzhou University, Fuzhou, Fujian 350116, China

[‡]College of Chemistry and Materials Science, Fujian Normal University, Fuzhou, Fujian 350117, China

[*]Corresponding Author: fengfu@fzu.edu.cn (F.-F Fu); 1959392119@qq.com (X. Zhang)

1. Main materials and apparatus

Pure xylose, glucose, galactose, maltose, fructose, sucrose and sodium citrate ($C_6H_5O_7Na_3 \cdot 2H_2O$) were purchased from Sangon Biotech Co., Ltd (Shanghai, China). The sodium borohydride ($NaBH_4$), acetic acid (CH_3COOH), sodium acetate ($CH_3CO_2Na \cdot 3H_2O$), trichloroacetic acid, acetonitrile and chloroform were obtained from Aladdin Company (Shanghai, China). 3,3',5,5'-Tetramethylbenzidine (TMB) were purchased from Shanghai Titan Technology Co., Ltd (China). All reagents are of analytical grade or ultrapure grade, and were used without any further purification. The water used in the experiment is Milli-Q water (18.2 MΩ·cm), which was prepared with Millipore pure system.

A Talos F200S G2 field transmission electron microscopy (TEM) (FEI, Netherlands) together with an energy dispersive X-ray spectroscopy (EDX) was used to obtain TEM images and EDX mapping. The X-ray diffraction (XRD) analysis was carried out with a Ultima IV X-ray diffractometer (Rigaku, Japan). The UV-visible spectrometry was performance with an Infinite 200 Pro microplate reader (Tecan, Switzerland). An Esca Lab 250 X-ray photoelectron spectrometer (XPS, Thermo Fisher Scientific Company, USA) was used for the X-ray photoelectron spectroscopy (XPS) analysis.

Table S1: Comparison on the apparent Michaelies-Menten constant (K_m) and maximum reaction rate (V_{max}) among AuNPs@MoS_2 dual-active nanozyme, HRP and GOx.

	Substrate	K_m (mM)	V_{max} (mol/L s)
AuNPs@MoS_2	H_2O_2	1.31	1.36×10^{-6}
HRP	H_2O_2	1.01	2.66×10^{-6}
AuNPs@MoS_2	TMB	0.044	5.60×10^{-8}
HRP	TMB	0.079	1.27×10^{-7}
AuNPs@MoS_2	Glucose	0.448	5.80×10^{-7}
GOx	Glucose	0.646	9.87×10^{-7}

Table S2: Analytical performances of the developed bio-enzyme-free colorimetric methods for the detection of glucose, xylose and galactose based on AuNPs@MoS_2

Analyte	Equation	Linear range	Visual LOD	Spectrometry LOD	RSD (n=5)
Glucose	$A_{652}=0.2699\times C + 0.1178$	0.0 - 0.7 mM	0.3 mM	11.0 μM	4 % (detecting 0.3 mM glucose)
Xylose	$A_{652}=0.3825\times C + 0.1077$	0.0 - 0.7 mM	0.3 mM	8.0 μM	3% (detecting 0.3 mM xylose)
Galactose	$A_{652}=0.6187\times C + 0.0980$	0.0 - 0.5 mM	0.2 mM	5.0 μM	2% (detecting 0.2 mM galactose)

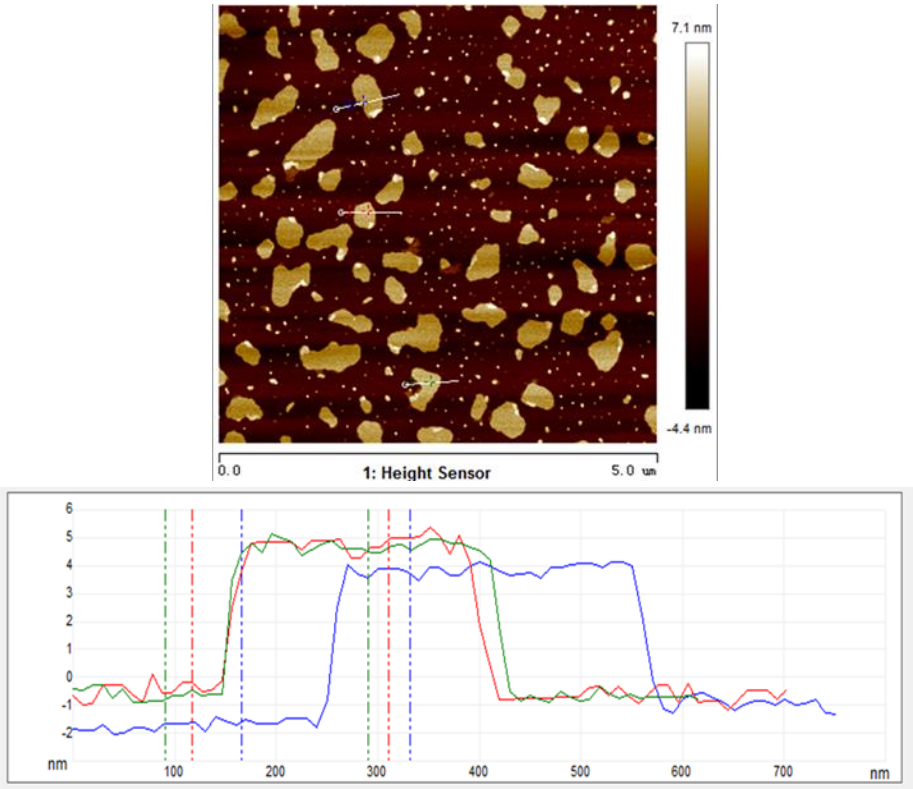

Figure S1: The AFM analysis of the MoS_2 nanosheets, which used to prepare AuNPs@MoS_2 nanozyme.

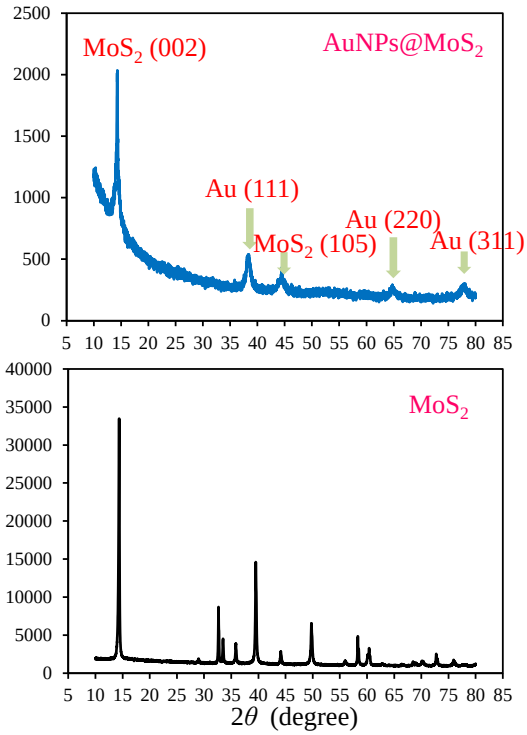

Figure S2: The XRD spectra of MoS_2 used to prepare MoS_2 nanosheets and the prepared AuNPs@MoS_2 nanozyme.

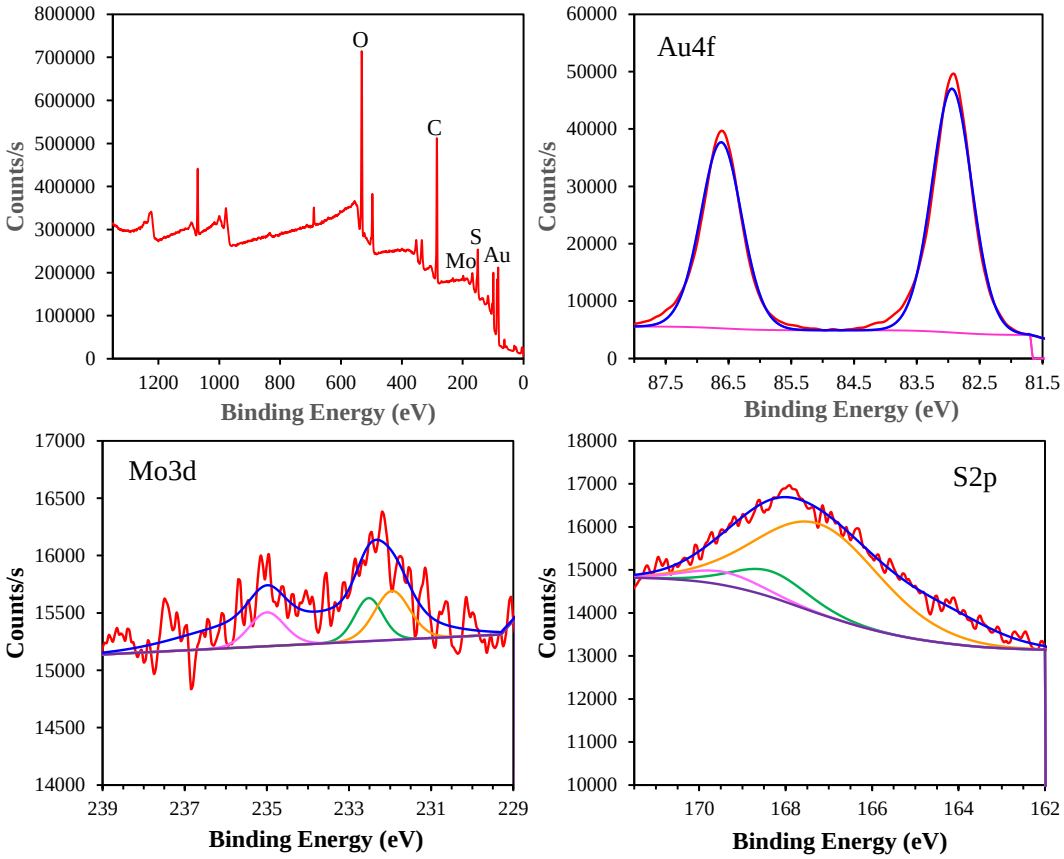

Figure S3: The X-ray photoelectron spectroscopy (XPS) analysis of the prepared AuNPs@MoS_2 nanozyme.

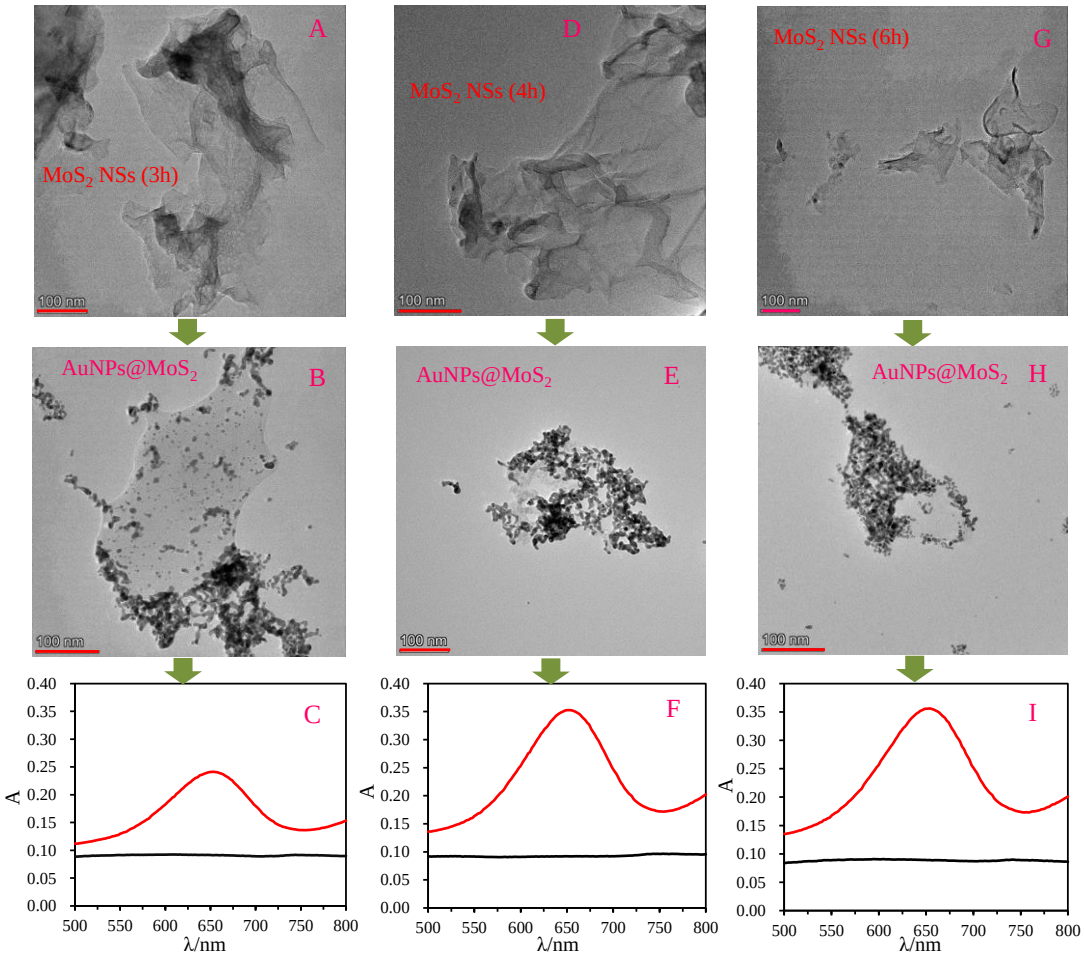

Figure S4: The TEM image of the prepared MoS_2 nanosheets under different time of ultra-sonication and the corresponding AuNPs@MoS_2 nanozyme, and the dual enzyme-like activities characterization of the prepared AuNPs@MoS_2 nanozyme. 3 hours (A, B, C), 4 hours (D, E, F) and 5 hours (G, H, I). The dual enzyme-like activities characterization was performed by directly using AuNPs@MoS_2 to catalyze the tandem reactions of glucose oxidation and H_2O_2-mediated oxidation of TMB, according to the procedure of 2.4 in experimental section. The concentration of glucose is 2.0 mM.

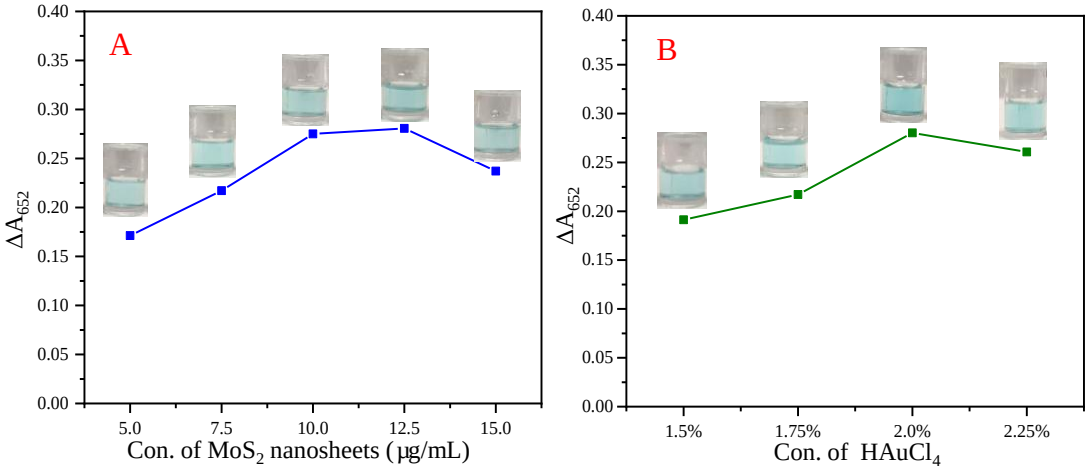

Figure S5: The effect of MoS_2 nanosheet concentration on the dual enzyme-like activities of the prepared AuNPs@MoS_2 nanozyme (A); the effect of $HAuCl_4$ concentration on the dual enzyme-like activities of the prepared AuNPs@MoS_2 nanozyme (B). The dual enzyme-like activities characterization was performed by directly using AuNPs@MoS_2 to catalyze the tandem reactions of glucose oxidation and H_2O_2-mediated oxidation of TMB, according to the procedure of 2.4 in experimental section. The concentration of glucose is 2.0 mM.

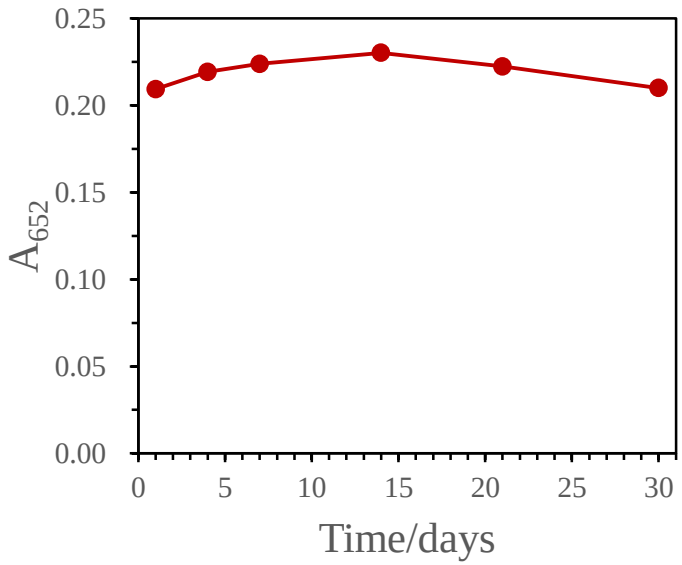

Figure S6: The variation of absorbance at 652 nm for detecting 0.5 mM glucose by using AuNPs@MoS_2, which was stored at 5 ℃ for different days. Data was obtained under the optimal selection of glucose detection method described in text.

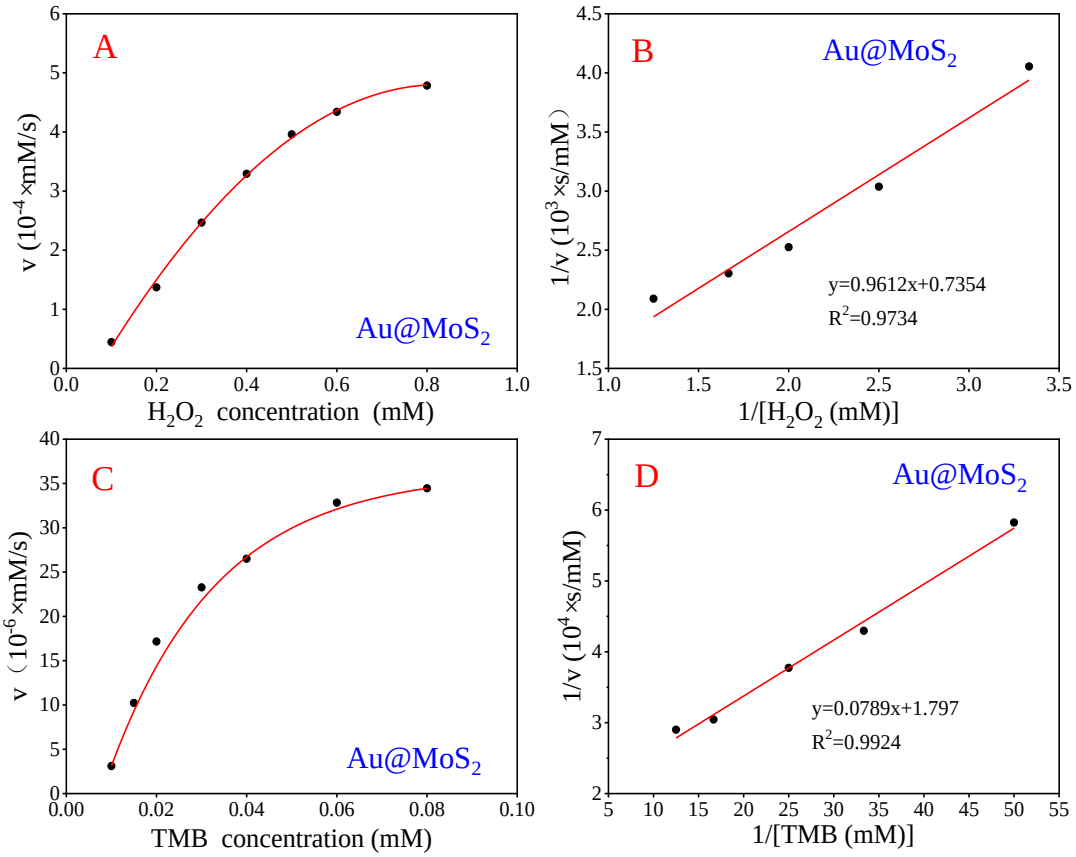

Figure S7: Steady-state kinetic analysis of AuNPs@MoS_2 as HRP mimics. The velocity of the reaction was measured by using 50 μL of AuNPs@MoS_2 in acetic acid/sodium acetate buffer (200 mM, pH 4.6) with a total volume of 200 μL. A: The time-reaction velocity variation of H_2O_2 under 0.1 mM of TMB; B: Double reciprocal plots of velocity versus H_2O_2 concentration at 0.1 mM TMB; C: The time-reaction velocity variation of TMB under 1.0 mM of H_2O_2; D: Double reciprocal plots of velocity versus TMB concentration at 1.0 mM H_2O_2.

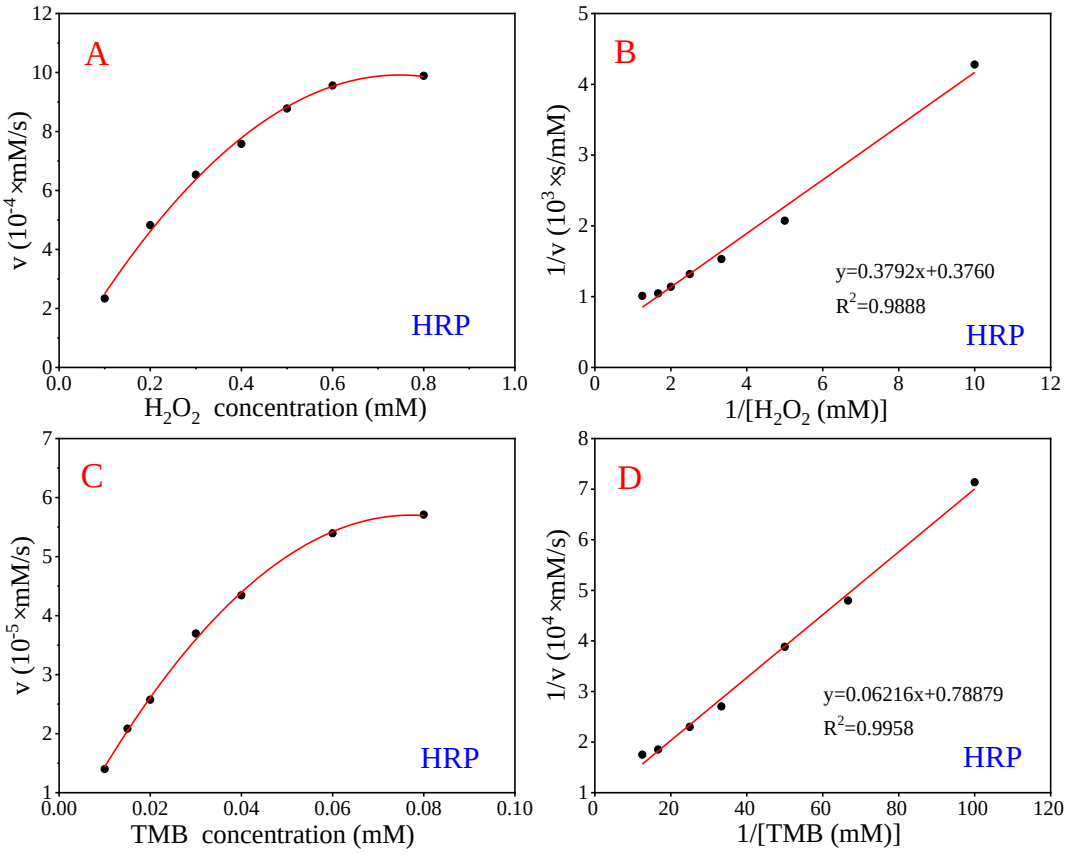

Figure S8: Steady-state kinetic analysis of natural HRP. The velocity of the reaction was measured by using 0.5 ng/mL of HRP in acetic acid/sodium acetate buffer (200 mM, pH 4.6). A: The time-reaction velocity variation of H_2O_2 under 0.1 mM of TMB; B: Double reciprocal plots of velocity versus H_2O_2 concentration at 0.1 mM TMB; C: The time-reaction velocity variation of TMB under 1.0 mM of H_2O_2; D: Double reciprocal plots of velocity versus TMB concentration at 1.0 mM H_2O_2.

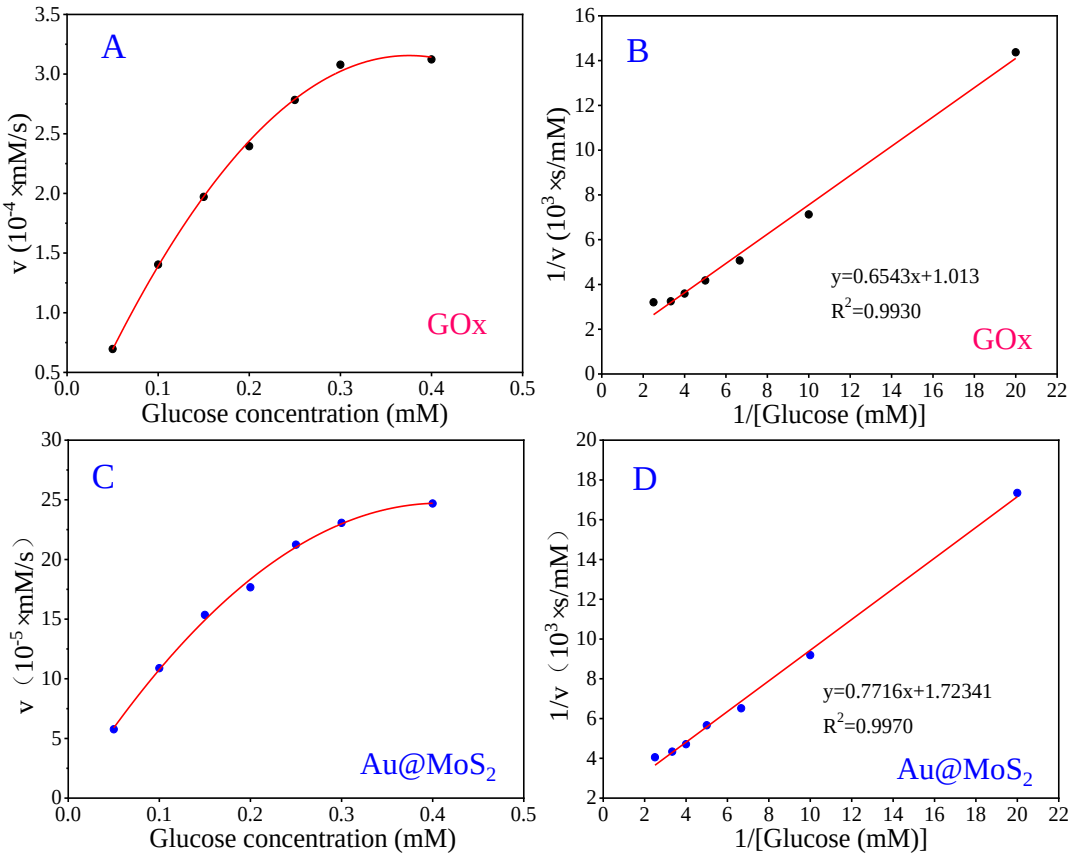

Figure S9: Steady-state kinetic analysis of natural GOx and AuNPs@MoS_2 as GOx mimics. The velocity of the reaction was measured in acetic acid/sodium acetate buffer (200 mM, pH 4.6). The concentration of HRP is 15 μg/mL, and the amount of AuNPs@MoS_2 is 60 μL in a total volume of 200 μL. A: The time-reaction velocity variation of glucose under GOx catalysis; B: Double reciprocal plots of velocity versus glucose concentration under GOx catalysis; C: The time-reaction velocity variation of glucose under AuNPs@MoS_2 catalysis; D: Double reciprocal plots of velocity versus glucose concentration under AuNPs@MoS_2 catalysis.

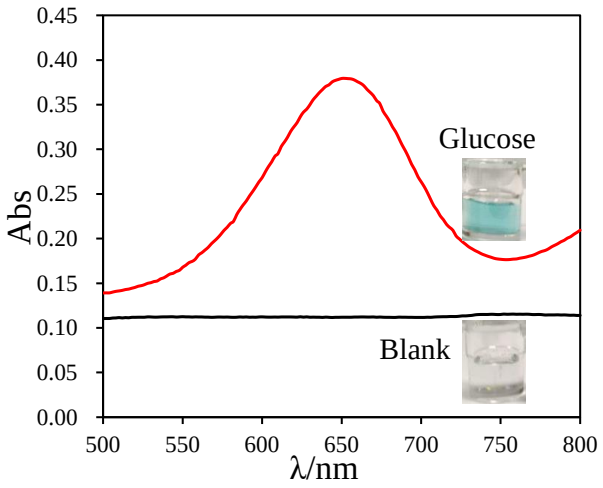

Figure S10: The photographs and absorption spectra of TMB solution in the presence of AuNPs@MoS_2 nanozyme together with glucose and AuNPs@MoS_2 without glucose (blank). The concentration of glucose is 2.0 mM.

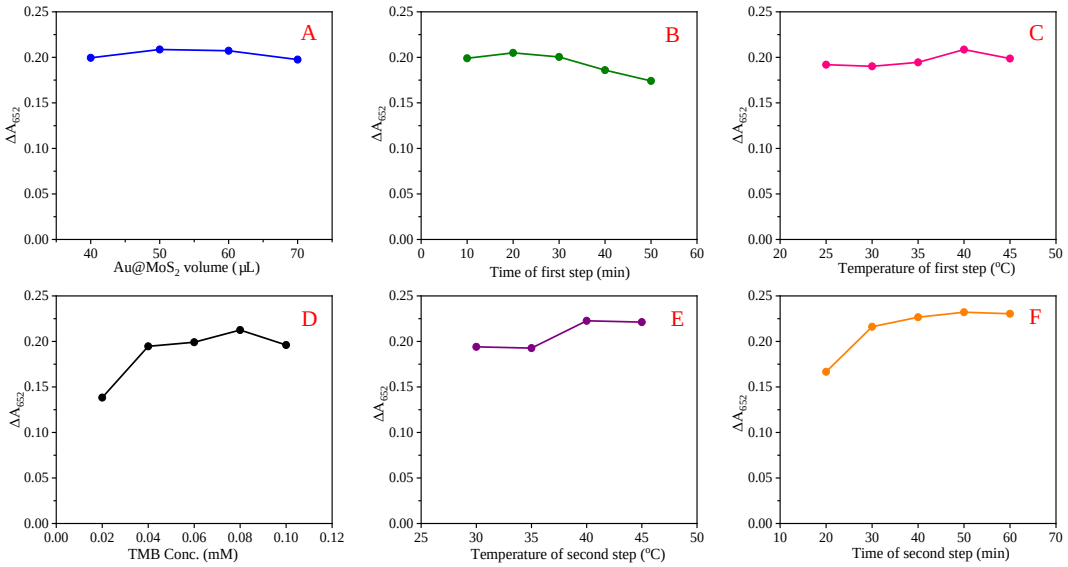

Figure S11: The effect of AuNPs@MoS_2 volume (A), the reaction time (B) and temperature (C) between AuNPs@MoS_2 and glucose, TMB concentration (D), and the reaction temperature (E) and time (F) between AuNPs@MoS_2 and TMB on the sensitivity of the method for the detection of glucose. Data were obtained under the optimal selection described in text except that will be optimized. The concentration of glucose is 1.0 mM.

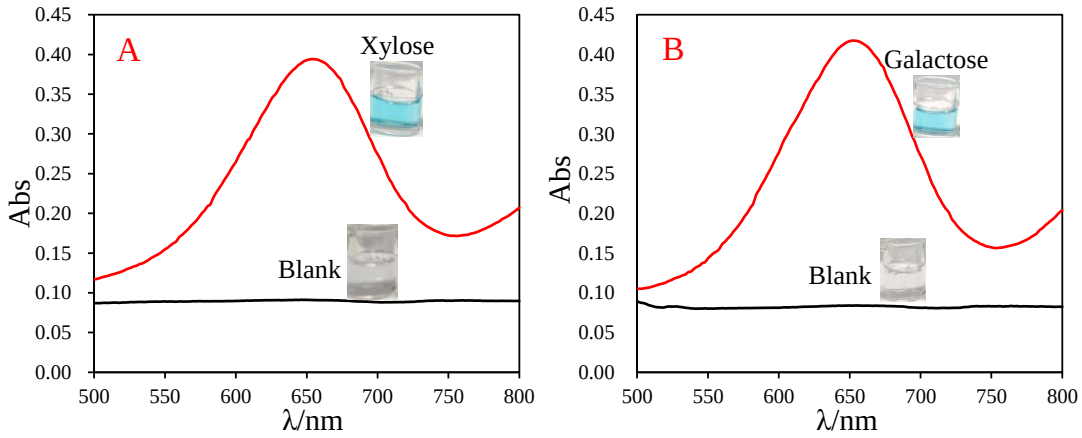

Figure S12: The photographs and absorption spectra of TMB solution in the presence of AuNPs@MoS_2 nanozyme together with xylose (A) or galactose (B), and AuNPs@MoS_2 without xylose or galactose (blank in A and B). The concentration of xylose or galactose is 2.0 mM.

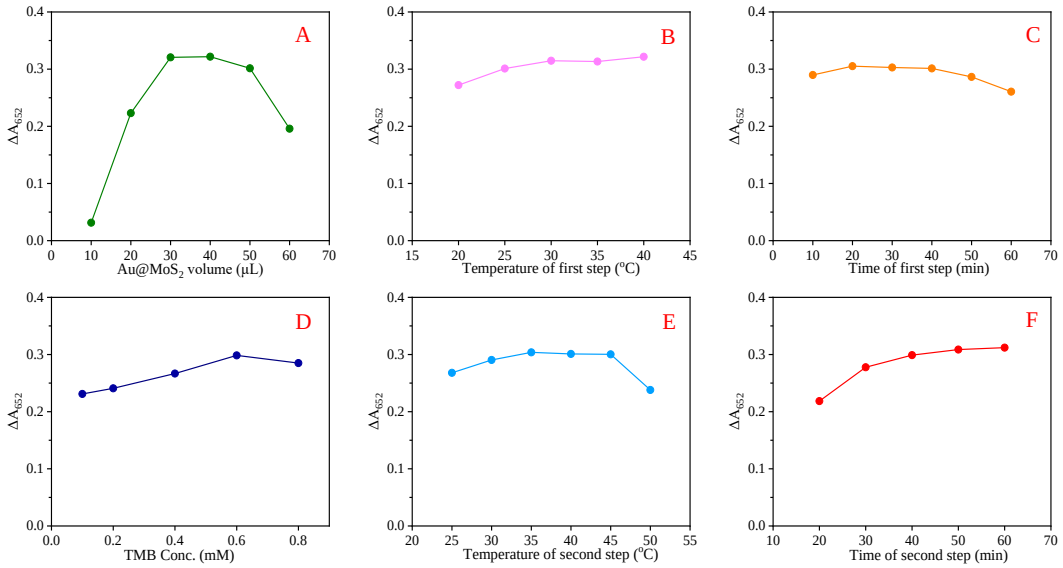

Figure S13: The effect of AuNPs@MoS_2 volume (A), the reaction temperature (B) and time (C) between AuNPs@MoS_2 and xylose or galactose, TMB concentration (D), and the reaction temperature (E) and time (F) between AuNPs@MoS_2 and TMB on the sensitivity of the method for the detection of xylose or galactose. Data were obtained under the optimal selection described in text except that will be optimized. The concentration of xylose or galactose is 2.0 mM.